STABLE PROTON BEAM ACCELERATION FROM A TWO-SPECIE ULTRATHIN FOIL TARGET*

Tong-Pu Yu†, Institut für Theoretische Physik I, HHUD, 40225 Düsseldorf, Germany
Department of Physics, National University of Defense Technology, Changsha 410073, China
Alexander Pukhov, Min Chen, Institut für Theoretische Physik I, HHUD, 40225 Düsseldorf, Germany

Abstract

By using multi-dimensional particle-in-cell simulations, we investigate the stabilization of proton beam acceleration in a two-specie ultra-thin foil. In this two-specie regime, the lighter protons are initially separated from the heavier carbon ions due to their higher charge-to-mass ratio Z/m. The laser pulse is well-defined so that it doesn't penetrate the carbon ion layer. The Rayleigh-Taylor-like (RT) instability seeded at the very early stage then only degrades the acceleration of the carbon ions which act as a "cushion" for the lighter protons. Due to the absence of proton-RT instability, the produced high quality mono-energetic proton beams can be well collimated even after the laser-foil interaction concludes.

INTRODUCTION

Recently, with the rapid development of laser technology, one of the most straightforward acceleration mechanisms, radiation pressure acceleration (RPA) [1] (also called laser piston or light sail), is being re-visited. The first RPA experiment [2] performed recently observed the ion acceleration in a phase-stable way [3] by the laser radiation pressure. However, the undesirable transverse Rayleigh-Taylor-like (RT) instability remains unavoidable. It develops gradually and finally leads to the transverse disruption of the foil. Unlike the electron acceleration in the bubble regime [4], a stable proton beam acceleration in the realistic three-dimensional (3D) geometry is unaccessible up to now.

In this paper, we report on a scheme to smoothly extend the 1D RPA model to multi-dimensional cases by using a two-specie ultrathin shaped foil. We found that this specially-prepared foil with the heavier carbon ions and the lighter protons can not only effectively avoid the foil deformation, but also significantly suppress the RT instability in case the laser intensity and the foil composition are carefully defined. The stabilization of the proton-RT instability can be attributed to two points: Firstly, both species are completely separated from each other at the very early stage. Secondly, the heavier carbon ions act as a "cushion" for the proton acceleration because the laser pulse directly interacts with the carbon ions but never reaches the proton layer. In the following, we firstly show the 1D RPA model in the two-specie regime and then discuss how to extend it to multi-dimensional cases.

* Work supported by GRK 1203 and TR18.

† Tongpu.Yu@tp1.uni-duesseldorf.de

TWO-SPECIE RPA MODEL AND 1D SIMULATION RESULTS

We start with the semi-analytical RPA model [5]. For a two-specie ultra-thin foil, we simply assume that the entire target keep intact during the acceleration and the target motion can thus be described as following:

$$\rho\frac{d(\gamma\beta)}{dt} = \frac{{E_L}^2}{2\pi c}\frac{1-\beta}{1+\beta}, \tag{1}$$

where $\rho = \sum m_i n_i L$ is the target area mass density, m_i, n_i, and L are the ion mass, ion density, and foil thickness, respectively. E_L represents the laser electric field. Obviously, the foil dynamics in the two-specie RPA regime is defined by the area mass density ρ, not the detailed foil composition, which is very different from the collisionless shock wave acceleration in Ref. [6].

We carry out a set of 1D simulations to investigate the detailed acceleration process by using the fully relativistic electromagnetic PIC code VLPL [7]. In the fist case, the longitudinal length of the simulation box is $x = 60\lambda$ and totally 6×10^4 cells are employed so that it can resolve the expected density spike. Each cell contains about 100 particles. The target is 0.1λ long, located at $x = 10\lambda$ and composed of carbon ions and protons with the same density $71.42n_c$, which corresponds to an electron density $n_e = 500n_c$. A CP laser pulse with the wavelength $\lambda = 1\mu m$ is incident from the left boundary at $t = 0$. The laser intensity follows a trapezoidal profile (linear growth - plateau - linear decrease) in time. The dimensionless laser intensity is $a_0 = 100$ and the duration is $\tau_L = 16T_0$ ($1T_0 - 14T_0 - 1T_0$). Absorbing boundary condition is applied to both the field and particle boundaries.

Fig. 1(a) shows the laser intensity evolution. Here, the wave front of the laser pulse arrives at the foil surface at $t = 10T_0$. We can see that a part of the laser pulse is reflected by the target because of the high foil density. As expected, the foil is accelerated forward as a whole until the laser-foil interaction concludes at about $t = 45T_0$. Fig. 1(b) presents the distribution of the ion density and the acceleration field E_x. At fist, the electrons are pulled out by the $J \times B$ force and a strong charge separation field forms behind the foil. Due to the higher charge-mass ratio Z_i/m_i, the protons move much faster than the carbon ions so that they instantaneously separate from each other. Gradually, the ions experience different acceleration fields, as shown by the red spike in the figure. The acceleration

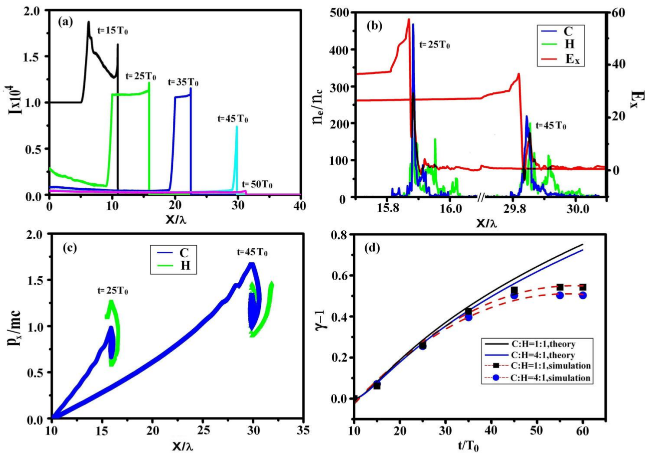

Figure 1: (Color online). (a) Laser intensity evolution. Here, $I = (E_y^2 + B_z^2)/2$ is normalized to $I_0 = 2.74 \times 10^{18} W/cm^2$. The laser-foil interaction ends at $t = 45T_0$. (b) Ion density distributions and the acceleration field E_x at $t = 25T_0$ and $45T_0$. Here, E_x is normalized to $E_0 = 3.2 \times 10^{12} V/m$. (c) Ion phase distribution at $t = 25T_0$ and $45T_0$. (d) Proton energy evolution from 1D PIC simulations (dashed line) and 1D RPA model (real line).

field inside the carbon layer is much higher than in the proton layer so that the carbons ions can be accelerated to catch up with the protons. The acceleration process repeats until $t = 45T_0$, similar to the "snow plow" in the electron acceleration. The fact that both heads of carbon ions and protons interlace with each other in phase space, as shown in Fig. 1(c), demonstrates the above acceleration process. Our simulation results agree well with the Ref. [3], where a typical "spiral structure" is observed in a pure Hydrogen foil.

The averaged proton energy evolution is shown in Fig. 1(d). At $t = 45T_0$, the proton energy is as high as $500MeV$, which is a little higher than the carbon ion energy $475MeV/u$. The proton energy doesn't increase anymore after the laser-foil interaction ends at $t = 45T_0$. Such high energies with a pronounced mono-energetic peak are unreachable in other ion acceleration regimes. For comparison, we also provide the theoretical calculation from Eq.(1) in the figure. Overall, they fit well with the simulation results without considering the limited laser duration. It is worthwhile to mention that the 1D models in Ref. [8] fail in our case. The final proton energies calculated from both models (hole-boring model and shock wave) are much lower than in our cases. This demonstrates that the RPA regime indeed dominates the ion acceleration in our case.

We also perform another simulation to check the influence of the foil composition on the proton acceleration, as shown in Fig. 1(d). In this case, we keep the electron density but vary the ratio of the ion densities $n_C : n_H$ from $1:1$ to $4:1$. That means that both cases have almost the same area mass density. All the other parameters are the same as in the first case. Obviously, the simulation results agree well with the predication of the 1D model. It demonstrates that the ion dynamics mainly depends on the area mass density, not the detailed foil composition.

2D SIMULATIONS

The 1D PIC simulation results above reveal that the RPA regime is a potentially promising ion acceleration mechanism. However, when we extend it to multi-dimensional cases, many problems occur. Firstly, the foil will be deformed by the incident laser pulses due to the inhomogeneous distribution of the laser intensity. This leads to a strong electron heating which will definitely pollute the final energy spectrum. Secondly, the ultrathin foil is very susceptible to the transverse instabilities, such as Rayleigh-Taylor-like (RT) instability [9] and Weibel instability [10]. Especially, the RT instability is seeded once the laser-foil interaction starts, and develops from the unstable interface at rate of a few laser cycles. Gradually, the foil surface becomes corrugated and pierced by the laser radiation and the entire target is torn into many clumps and bubbles [11]. Therefore, how to suppress the undesirable RT instability becomes a central problem. Thirdly, the ion acceleration in the RPA regime is usually accompanied by many other acceleration mechanisms, which makes the acceleration process more complicated and intractable.

In order to solve the foil deformation, we have to use a shaped foil target (SFT) [12] or a density-modulated foil target (DMFT) [13] to compensate for the inhomogeneous laser intensity distribution. Taking the normally used Gaussian laser pulses for example, the foil thickness or the density should be modulated by a well-matched Gaussian function $L_y = max[L_{max} exp(-y^2/\sigma_T^2), L_{cut}]$, where L_{max} is the maximal foil thickness, L_{cut} the cutoff thickness, and σ_T the spot radius. Following this way, we make sure that each L_y thickness layer acts as in the 1D case and the whole foil can be pushed forward as a whole. In following, we show the 2D simulation results by using such kind of target engineering.

The simulation box is $X \times Y = 50\lambda \times 50\lambda$, sampled by 10000×5000 cells. Each cell contains 100 particles in the plasma region. The foil is initially located at $x = 10\lambda$ with parameters $L_{max} = 0.1\lambda$, $L_{cut} = 0.05\lambda$, and $\sigma_T = 7\lambda$. Both ions have the same particle density $71.94n_c$ as in the 1D case above. A Gaussian laser pulse with the focal size $\sigma_L = 8\lambda$ is incident from the left boundary. The lase duration is $\tau_L = 10T_0(1T_0 - 8T_0 - 1T_0)$. All the other parameters are the same as in the 1D case.

The ion density distribution is shown in Fig. 2. At $t = 17.5T_0$, the protons have already been separated from the heavier carbon ions. Compared with the simulation results in a pure-Hydrogen case [11], the proton layer is well maintained during the acceleration. The laser-driven RT instability is significantly suppressed so that it can be collimated even after the laser-foil interaction concludes at $t = 25T_0$. On the contrary, the carbon ions are extensively spread in space. This can be attributed to the direct interac-

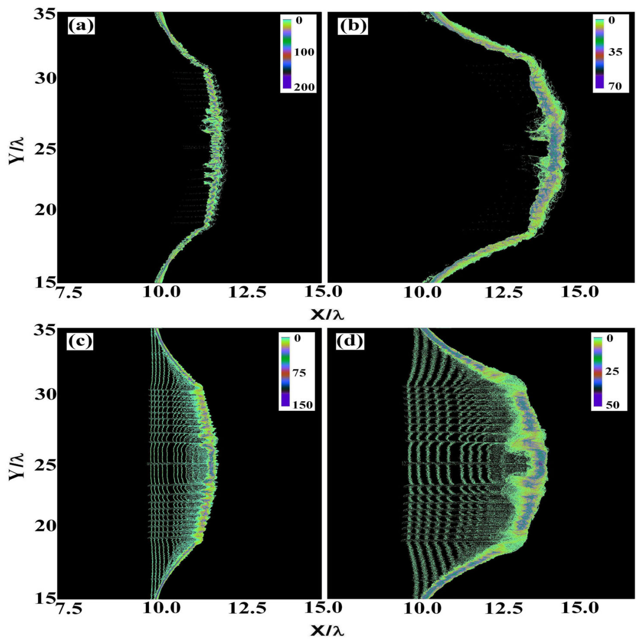

Figure 2: (Color online). Proton density distribution at (a) $t = 17.5T_0$ and (b) $22.5T_0$. The corresponding carbon ion density distribution is also presented in (c) and (d).

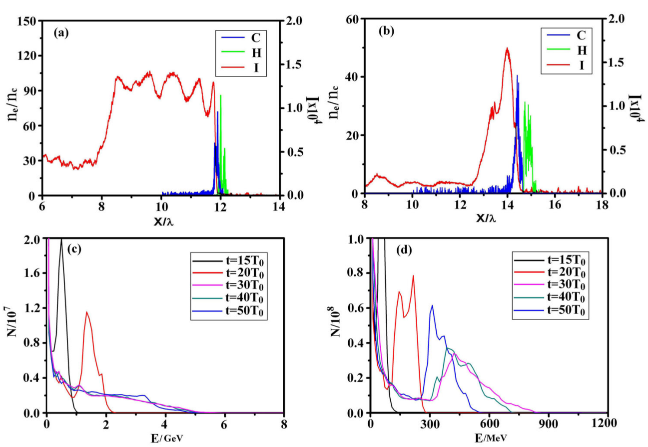

Figure 3: (Color online). The ion density distribution and the corresponding laser intensity along $y = 0$ at (a) $t = 17.5T_0$ and (b) $22.5T_0$. Here, I has the same definition as above. The energy spectrum evolutions of (c) carbon ions and (d) protons are also presented here.

tion of the carbon plasma with the laser pulses. As shown in Fig. 2 (d), the carbon-RT instability develops at a high rate so that it spreads in space soon. We can get a further understanding of the physics under the simulation results from Fig. 3 (a) and (b). It is clear that the laser pulse always hits only the carbon layer but never reaches the protons. Like the "snow plow" in the electron acceleration, the carbon ions in our case act as a "Cushion" or a "Buffer" for the proton acceleration.

The ion energy spectrum evolution is also presented in Fig. 3. As discussed above, the carbon ions have a widely-spread spectrum although a energy peak is observed at $t = 15T_0$ and $20T_0$. This is a typical result of RT instability. However, the protons always show a quasi-monoenergetic peak even at $t = 50T_0$. The total number of the particles within the energy $300 - 600MeV$ is up to 5.7×10^8. For a single-ion specie [1, 11], although a energy peak is formed initially, it lowers gradually and disappears soon, just as we observed in the carbon spectrum. Obviously, the energy spectrum in this two-specie case is significantly improved.

The stabilization of the proton-RT instability can be attributed to two facts: Firstly, they are initially separated from the carbon ions so that the RT instability can not reach the proton layer. Secondly, the the proton layer is always riding on the heavier carbon ions so that it avoid the RT instability. We can use a three-interface model to interpret it [14]. A detailed explanation with this model is to be published somewhere.

CONCLUSIONS

In conclusion, we investigate the detailed ion acceleration from an ultra-thin C-H foil by use of multi-dimensional PIC simulations. For the 2D cases, the carbon ions spread extensively in the space, showing a quasi-exponential spectrum but the protons always ride on the carbon ion front forming a high quality proton beam. The sharp front separating the species is well defined and the proton beam acceleration is very stable, which results from the significant suppression of the RT instability in the compact proton layer. Benefiting from the superpower lasers such as HiPER and ELI, the stable acceleration mechanism described above may be demonstrated by experiments and has a potential to be applied in the near future.

We acknowledge the finical support from DAAD via Kongress- und Vortragsreisenprogramm.

REFERENCES

[1] F. Pegoraro, *et al.*, Phys. Rev. Lett. **99**, 065002 (2007).

[2] A. Henig, *et al.*, Phys. Rev. Lett. **103**, 245003 (2009).

[3] X. Q. Yan, *et al.*, Phys. Rev. Lett. **100**, 135003 (2008).

[4] A. Pukhov *et al.*, Appl. Phys. B **74**, 355 (2002).

[5] V. K. Tripathi, *et al.*, Plasma Phys. Control. Fusion **51**, 024014 (2009).

[6] L. Ji, *et al.*, Phys. Rev. Lett. **101**, 164802 (2008).

[7] A. Pukhov, J. Plasma Phys. **61**, 425 (1999).

[8] A. P. L. Robinson, *et al.*, Plasma Phys. Control. Fusion **51** 095006 (2009); X. Zhang, *et al.*, Phys. Rev. ST Accel. Beams **12**, 021301 (2009).

[9] F. Pegoraro, *et al.*, Eur. Phys. J. D **55**, 399-405 (2009).

[10] E. S. Weibel, Phys. Rev. Lett. **2**, 83 (1959).

[11] X. Q. Yan, *et al.*, Phys. Rev. Lett. **103**, 135001 (2009).

[12] M. Chen, *et al.*, Phys. Rev. Lett. **103**, 024801 (2009).

[13] T. P. Yu, *et al.*, Laser Part. Beams **27**, 611-617 (2009).

[14] T. P. Yu, *et al.*, submitted (2009).